Journal of Molecular Liquids 417 (2025) 126655

Contents lists available at ScienceDirect

Journal of Molecular Liquids

journal homepage: www.elsevier.com/locate/molliq

Thermophysical characterization of lidocaine:camphor:thymol or l-menthol eutectic mixtures: Experimental and modelling

Mónica Sancho-Blasco [a], Jorge L. Pastor [a], José Muñoz-Embid [a,b], Carlos Lafuente [a,b], Manuela Artal [a,b,*]

[a] Departamento de Química Física, Facultad de Ciencias, Universidad de Zaragoza, Zaragoza, Spain
[b] Instituto Agroalimentario de Aragón - IA2 (Universidad de Zaragoza - CITA), Zaragoza, Spain

ARTICLE INFO

Keywords:
Lidocaine
Camphor
Thymol
L-menthol
Therapeutic eutectic solvents
Thermodynamic and transport Properties

ABSTRACT

Knowing the values of the thermodynamic and transport properties of fluids is essential for their implementation in different fields. In addition, their analysis allows us to understand the intermolecular interactions which is useful in the subsequent design of processes. In this work, two ternary eutectic mixtures composed of lidocaine, camphor, and thymol or l-menthol were studied. Six thermophysical properties were measured at 0.1 MPa and at various temperatures. Density values up to 65 MPa were also determined. From these data, different properties were calculated, such as isobaric expansibility, isentropic and isothermal compressibility, internal pressure, and critical temperature, among others. The mixture with thymol was the most dense, structured, and viscous. The correlations and models used showed small deviations between the experimental and estimated values. The deviations of the density and isobaric molar heat capacity predicted with PC-SAFT equation of state were lower than 1.4 % and 3.1 %, respectively. The interactions between lidocaine and thymol were the strongest. On the other hand, camphor was shown to be a steric hindrance to binary interactions.

1. Introduction

Healthcare challenges require innovative, sustainable, effective, and affordable pharmaceutical solutions. Despite major advances in research in this field, two major obstacles remain to be overcome. First, almost 40 % of drugs marketed or in development exhibit reduced solubility. This fact is often offset by higher doses increasing costs and increased risk of side effects [1,2]. Second, the increasing number of approved biological therapies (peptides, proteins, or nucleic acids), brings additional challenges for their stability, storage, and administration, including the advantages of the formulations in liquid phase [3,4]. Recently, the use of deep eutectic solvents (DESs) in pharmacology is being postulated as an alternative with multiple advantages. Briefly, DESs are mixtures of two or more components that show a much lower melting point when combined so that they are in liquid phase at room temperature. Although the term eutectic was introduced in 1884 [5], the work published by Abbott et al. [6] in 2004 is considered as the starting point of this field. Since then, DESs have attracted great attention in very distant scientific areas, ranging from structural biology to energy storage materials, since it is possible to tailor their physicochemical properties, such as hydrophobicity, ionic strength, acid/base character or dielectric constant, among others. A more exhaustive analysis of their definition and typology can be found in several reviews [7–11]. In principle, any compound capable of donating or accepting hydrogen bonds can be component of DES. Most active pharmaceutical ingredients (APIs) meet this requirement and can therefore give rise to mixtures that will also have therapeutic properties. In this case, they are called THEDESs. They have gained relevance in the pharmaceutical context due, among other things, to the synergies detected between the constituent APIs thus enhancing the value of the final product [10,12–14].

Lidocaine (L) is one of the most widely used APIs in the design and preparation of THEDESs due to its anesthetic, antiarrhythmic, and antiepileptic activity [15]. Its combination with prilocaine (known as EMLA®) was the first DES marketed in 1949 [16]. Later, other binary mixtures with nonsteroidal carboxylic acid anti-inflammatories or terpenes were evaluated [17–20]. This work presents the thermophysical characterization of two ternary mixtures of L with camphor (C) and thymol (T) or l-menthol (M). Previously, the structural study of these mixtures was carried out and published by us. This work showed the presence of important intermolecular interactions between lidocaine

* Corresponding author at: Departamento de Química Física, Facultad de Ciencias, Universidad de Zaragoza, Zaragoza, Spain.
E-mail address: martal@unizar.es (M. Artal).

https://doi.org/10.1016/j.molliq.2024.126655
Received 21 September 2024; Received in revised form 29 November 2024; Accepted 30 November 2024
Available online 1 December 2024

Table 1
Compounds used in this work.

Chemical (Acronym)	CAS No	Purity [a]	M/g·mol^{-1}	Structure
Lidocaine (L)	137–58-6	>0.98	234.34	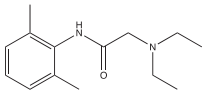
Camphor (C)	464–49-3	>0.98	152.23	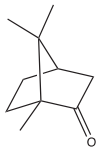
Thymol (T)	89–83-8	>0.985	150.22	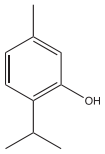
L-menthol (M)	89–78-1	>0.99	156.27	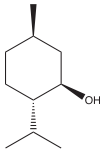

[a] As stated by the supplier (mass fraction).

Table 2
Summary of the devices used in the thermophysical characterization at $p = 0.1$ MPa.

Property	Devices	$u(T)$/K	$U_c(Y)$ [a]	$MRD(Y)$ [b]/%
Density,ρ	Oscillating U-tube density meter, Anton Paar DSA 5000 [c]	0.005	0.05 kg·m^{-3}	0.004
Speed of sound,u	Acoustic, time-of-flight method, Anton Paar DSA 5000 [c]	0.005	0.5 m·s^{-1}	0.026
Refractive index,n_D	Standard Abbe refractometer, Abbemat-HP refractometer Dr. Kernchen [d]	0.01	2·10^{-5}	0.007
Isobaric molar heat capacity,$C_{p,m}$	Differential scanning calorimeter, TA Instruments DSC Q2000	0.5	1 %	0.028
Surface tension,γ	Drop volume tensiometer, Lauda TVT-2 [d]	0.01	1 %	0.21
Kinematic viscosity,ν	Capillary viscosimeter Ubbelohde, Schoot-Geräte AVS-440	0.01	1 %	0.28

[a] $k = 2$ (0.95 level of confidence); [b] $MRD(Y) = \frac{100}{n}\sum_{i=1}^{n}\left|\frac{Y_{i,lit} - Y_{i,exp}}{Y_{i,exp}}\right|$, [c] Calibrated with dry air and water MilliQ ($\rho = 18.2\ \mu$ S·cm^{-1}); [d] Calibrated with water MilliQ ($\rho = 18.2\ \mu$ S·cm^{-1}).

and terpenes [20]. The three compounds enhance transdermal penetration, which is why their use in medicinal and cosmetic applications is widespread. Other benefits such as their activity against microbes or fungi, and their power to stimulate thermoregulatory receptors have been reported [20]. The structures of T and M differ only in that the cycle of the first is of an aromatic type. Nevertheless, this fact can have a great influence on their behavior. The results of this work will allow us to further investigate the intermolecular interactions present in both mixtures based on the differences observed in their properties. In addition, previous studies carried out on the corresponding binary mixtures [19–21] will allow us to analyze the effect of the addition of the third component. For the ternary mixtures, no literature data was found. From an operational point of view, the use of correlations and thermodynamic models that are capable of calculating and predicting the values of thermophysical properties in a wide range of conditions (pressure, temperature, and composition) is very important in the industry. Nevertheless, they must be previously validated. In the following, we obtain the coefficients that allow calculating the value of the properties at any pressure and temperature within the working range of this study. We also show the goodness of correlations such as Taherzadeh et al. [22], Gugghenheim [23], Eotvos [24], Papazian [25], Pelofsky and Mukherjee [26], that allow estimating the isobaric molar heat capacity, critical temperature, and surface tension. Finally, we validate the PC-SAFT equation of state [27,28] as a predictive thermodynamic model.

This article will focus on the measurement and evaluation of thermodynamic and transport properties at 0.1 MPa of two ternary lidocaine-based eutectic mixtures. Also, density data up to 65 MPa were determined. The lowest working temperature was 278.15 K in the equipment operating at atmospheric pressure, and 283.15 K in the high-pressure device. The highest temperature was 338.15 K in all cases. From all these values, different derived properties were calculated and several correlations were applied. In addition, the PC-SAFT equation of state was validated for both mixtures in a wide range of pressure and temperature.

2. Experimental section

2.1. Materials

The characteristics and structures of the pure compounds used in this work are listed in Table 1. All of them were provided by Sigma–Aldrich and no purification processes were applied. The mixtures were made by weighing (PB210S Sartorius balance) the appropriate mass of each compound to obtain the chosen molar fraction. The standard uncertainty in the weight was of $u(m) = 1{\cdot}10^{-4}$ g. Stirring and heating at 323 K were then applied simultaneously until a homogeneous liquid was obtained. The water content was measured with an automatic titrator Crison KF 1S-2B and the value was less than 300 ppm in all cases. Finally, the eutectic mixtures were kept at 298 K until used. The studied mixtures were lidocaine:camphor:l-menthol (1:1:2, molar ratio) and lidocaine:camphor:thymol (1:1:1, molar ratio) and are called through the manuscript as LCM2 and LCT, respectively. The molar masses (M) were estimated from the molar mass of each compound (M_i) and its molar fraction (x_i) as $M = \sum_i x_i M_i$. The values were M(LCM2) = 174.78 g·mol^{-1}, and M(LCT) = 178.93 g·mol^{-1}.

2.2. Apparatus

The thermophysical characterization at $p = 0.1$ MPa was carried out with widely known devices. Table 2 reports the type of apparatus, the standard uncertainty in the temperature ($u(T)$), the combined expanded uncertainties for each property ($U_c(Y)$), and the mean relative deviations ($MRD(Y)$) obtained from checking it with benzene. For all properties, each tabulated data was the average of two replicates with a coefficient of variation less than the experimental uncertainty. Furthermore, for each replicate of the surface tension, 6 cycles of 6 drops per cycle were averaged. Dynamic viscosity (η) was calculated from density and kinematic viscosity data, $\eta = \rho\nu$.

The measurement of density under pressure was performed with a

thermostatted oscillating U-tube density meter (Anton Paar DMA HP 5000). A hand pump 750.1100 (Sitec) was used to achieve the working pressure that was measured with a transducer US181 (Measuring Specialties). The device was calibrated with dry air, hexane, water MilliQ (ρ = 18.2 μ S·cm^{-1}), and dichloromethane. Later, it was verified with toluene. The values of the standard uncertainties in the temperature and pressure, combined expanded uncertainty (k = 2 (0.95 level of confidence) in the density, and mean relative deviation in the checking were $u(T)$=±0.01 K, $u(p)$=±0.05 MPa, $U_c(\rho)$=±0.01 kg·m^{-3}, and$MRD(\rho)$ = 0.01 %.

3. Model and correlations

3.1. PC-SAFT EoS

This model, developed by Gross and Sadowski [27,28] is widely used in the literature for all types of fluids. It is based on the considering the Helmholtz energy ($\tilde{a}$) as the sum of an ideal gas contribution ($\tilde{a}^{id}$) and a residual ($\tilde{a}^{res}$). A repulsive term described using the hard-chain reference system ($\tilde{a}^{hc}$), and several attractive ones as the dispersive ($\tilde{a}^{dis}$) and association ($\tilde{a}^{assoc}$) contribute to the residual term.

$$\tilde{a}^{res} = \tilde{a}^{hc} + \tilde{a}^{dis} + \tilde{a}^{assoc} \tag{1}$$

The equations of the three summands are [29–31]:

$$\tilde{a}^{hc} = m\tilde{a}^{hs} - (m-1)\ln g^{hs} \tag{2}$$

$$\tilde{a}^{dis} = -2\pi\rho m^2\left(\frac{\varepsilon}{kT}\right)\sigma^3\sum_{i=0}^{6}\left[a_{0i}+\frac{m-1}{m}a_{1i}+\frac{m-1}{m}\frac{m-2}{m}a_{2i}\right]\eta^i - \pi\rho mkT\left(\frac{\partial\rho}{\partial p}\right)_{hc} m^2\left(\frac{\varepsilon}{kT}\right)^2\sigma^3\sum_{i=0}^{6}\left[b_{0i}+\frac{m-1}{m}b_{1i}+\frac{m-1}{m}\frac{m-2}{m}b_{2i}\right]\eta^i \tag{3}$$

$$\tilde{a}^{assoc} = \sum_A\left[\ln\left(1+\rho X^A\Delta\right)^{-1} - \frac{\left(1+\rho X^A\Delta\right)^{-1}}{2}\right] + \frac{1}{2}S \tag{4}$$

$$\Delta = \kappa^{A_iB_i}\sigma^3 g^{hs}\left[\exp\left(\frac{\varepsilon^{A_iB_i}}{kT}\right)-1\right] \tag{5}$$

where m is the chain segment number, g^{hs} is the radial pair distribution function of the segments, $\tilde{a}^{hs}$ is the Helmholtz energy of the hard sphere, ρ is the density, p is the pressure, T is the temperature, σ is the segment diameter, ε is the segment energy, η is the packing fraction, X^A is the fraction of unbonded monomers, Δ is the tendency to form n-mers, $\kappa^{A_iB_i}$ is the association volume, $\varepsilon^{A_iB_i}$ is the association energy, and S is the number of associated sites of the compound. The parameters a_{0i}, a_{1i}, a_{2i}, b_{0i}, b_{1i}, and b_{2i} are called *universal constants* and were obtained from the optimization of the thermodynamic properties of n-alkanes.

In summary, three geometrical parameters (m, σ and ε) are needed to characterize each pure compound in this model. Also, two additional ($\kappa^{A_iB_i}$ and $\varepsilon^{A_iB_i}$) parameters and an association scheme must be provided for substances able to associate. In the case of mixtures, mixing rules are needed and we have used the following:

$$\sigma_{ij} = \left(\sigma_i+\sigma_j\right)/2 \tag{6}$$

$$\varepsilon_{ij} = \sqrt{\varepsilon_i\varepsilon_j}\left(1-k_{ij}\right) \tag{7}$$

$$\kappa^{A_iB_j} = \sqrt{\kappa^{A_iB_i}\kappa^{A_jB_j}} \tag{8}$$

$$\varepsilon^{A_iB_j} = \left(\varepsilon^{A_iB_i}+\varepsilon^{A_jB_j}\right)/2 \tag{9}$$

where the subscripts i and j refer to each of the compounds present in the mixture. A no-null binary interaction parameter (k_{ij}) can be estimated from the thermodynamic properties of the mixture. In this way, the model loses the predictive character and becomes a correlation.

3.2. Correlations

3.2.1. Properties (p = 0.1 MPa) – Temperature

For a range of temperatures such as the one studied here, the thermodynamic properties at$p$ = 0.1 MPa mostly show a linear correlation, ascending or descending, with T:

$$Y = A_Y + B_Y T \tag{10}$$

where Y is $\rho, u, n_D, \gamma; A_Y$ and B_Y, are the fit parameters.

The effect of the temperature on the transport properties at$p$ = 0.1 MPa is more pronounced at low temperatures so they follow an exponential equation. We have used the VFT expression [32–34]:

$$\eta = A\exp\left(\frac{B}{T-C}\right) \tag{11}$$

where A, B, and C, are the fit parameters.

3.2.2. To estimate the isobaric molar heat capacity

A method to estimate the $C_{p,m}$ of eutectic mixtures was proposed by Taherzadeh et al. [22]. The equations are the following:

$$C_{p,m} = A + 132.27T^{1/4} \tag{12}$$

$$A = 3.8\bullet10^{-4}\frac{M^3}{p_c^6} + 6.3\bullet10^{-5}M^{2\omega} - \frac{24577.4}{M} - 94.9 \tag{13}$$

Where T is the temperature, M is the molar mass, p_c is the critical pressure, and ω is the acentric factor. The Lee-Kesler (LK) mixing rules extended to ternary mixtures [35] was used to calculate p_c and ω of both THEDEs as follows:

$$p_c(\text{bar}) = (0.2905 - 0.0850\omega)\frac{83.1447T_c}{V_c} \tag{14}$$

$$\omega = \sum_{n=1}^{3} x_n\omega_n \tag{15}$$

$$V_c(\text{mL/mol}) = \sum_{n=1}^{3}\sum_{m=1}^{3} x_n x_m V_{c,mn} \tag{16}$$

$$T_c(\text{K}) = \frac{1}{V_c^{0.25}}\sum_{n=1}^{3}\sum_{m=1}^{3} x_n x_m V_{c,mn}^{0.25} T_{c,mn} \tag{17}$$

$$V_{c,mn}(\text{mL/mol}) = \frac{1}{8}\left(V_{c,n}^{1/3} + V_{c,m}^{1/3}\right)^3 \tag{18}$$

$$T_{c,mn}(\text{K}) = \left(T_{c,n}T_{c,m}\right)^{0.5} \tag{19}$$

Where T_c and V_c are the critical temperature and critical volume of the THEDES. The subscripts n and m represent each component, and mn is the subscript indicating binary interaction term.

3.2.3. To estimate the critical temperature

The T_c can be calculated with thermodynamic models as in the previous sections (eq. 1–19). In addition, it can be obtained from data of γ and ρ at several T with the Gugghenheim [23] and Eötvos [24] equations:

$$\gamma = \gamma_0\left(1 - T/T_c\right)^{11/9} \tag{20}$$

$$\gamma(M/\rho)^{2/3} = K(T_c - T) \tag{21}$$

Table 3
Summary of the thermophysical properties at $T = 298.15$ K and $p =$ 0.1 MPa of the studied mixtures.

Property	lidocaine:camphor:l-menthol (1:1:2)	lidocaine:camphor:thymol (1:1:1)
Density ρ/kg·m^{-3}	939.69	979.76
Speed of sound u/m·s^{-1}	1395.69	1431.77
Refraction index n_D	1.47930	1.50637
Isobaric molar heat capacity $C_{p,m}$/J·mol^{-1}·K^{-1}	338	322
Surface tension γ/mN·m^{-1}	30.29	32.48
Dynamic viscosity η/mPa·s	25.70	54.34
Isobaric expansibility α_p/ kK^{-1}	0.799	0.778
Isothermal compressibility κ_T/ TPa^{-1}	660.98	601.75
Internal pressure π_T/ TPa^{-1}	360.53	385.26
Isentropic compressibility κ_s/ TPa^{-1}	546.31	497.89
Molar refraction R_m/ cm^3·mol^{-1}	52.77	54.29
Free volume f_m/ cm^3·mol^{-1}	133.22	128.33
Entropy of surface ΔS_S/ mN·m^{-1}·K^{-1}	0.0823	0.0860
Enthalpy of surface ΔH_S/ mN·m^{-1}	54.83	58.12
Activation energy of viscous flow $E_{a,\eta}$/ kJ·mol^{-1}	47.13	52.66

Standard uncertainties are: $u(T)$=0.005 K for density and speed of sound and 0.01 K for the rest of properties; $u(p)$=0.5 kPa. The combined expanded uncertainties (0.95 level of confidence, k=2) are$U_c(\rho) = 0.05$ kg·m^{-3}; $U_c(u)$=0.5 m·s^{-1}; $U_c(n_D)$=2·10^{-5}; $U_c(C_{p,m})$=1%; $U_c(\gamma)$=1%; $U_c(\eta)$=1%; $U_c(\alpha_p)$=0.04 kK^{-1}; $U_c(\kappa_T)$=0.22 TPa^{-1}; $U_c(\kappa_s)$=0.22 TPa^{-1}; $U_c(R_m)$=0.004 cm^3·mol^{-1}; $U_c(f_m)$=0.03 cm^3·mol^{-1}; $U_c(\Delta S_S)$=0.001 mN·m^{-1}·K^{-1}; $U_c(\Delta H_S)$=0.06 mN·m^{-1}.

Where γ_0 is the surface tension at 0 K.

3.2.4. To estimate the surface tension

The equation of Papazian [25] allows obtaining the values of γ from the dielectric constant (ε_s) data at similar p and T. Except to liquids with strong hydrogen bonds, the Maxwell relation ($n_D^2 = \varepsilon_s$) can be used and the correlation equation is:

$$\gamma = A\left(\frac{n_D^2 - 1}{2n_D^2 + 1}\right) + B \tag{22}$$

The equations of Pelofsky and Murkerjee [26] relate γ and η of a fluid at each T:

$$\ln\gamma = \ln A_1 + \frac{B_1}{\eta} \tag{23}$$

$$\ln\gamma = \ln A_2 + \frac{B_2}{3}\ln\eta \tag{24}$$

Where A_1, A_2, B_1, and B_2 are the fit coefficients.

3.2.5. Pressure – Density – Temperature

The equation of Tait was used to correlate p, ρ and T [36]. The expressions are:

$$\rho = \frac{\rho_0(T, p_0)}{1 - C \bullet \ln\left(\frac{B(T)+p}{B(T)+p_0}\right)} \tag{25}$$

$$\rho_0(T, p_0) = \sum_{i=0}^{n} A_i \cdot T^i \tag{26}$$

$$B(T) = \sum_{i=0}^{n} B_i \cdot T^i \tag{27}$$

where p_0 is the reference pressure (0.1 MPa) and ρ_0 is the density at p_0. The A_i, B_i, and C are the fitted parameters. From $p\rho T$ data and by deriving of eq. (20), several properties can be obtained. They are the isobaric thermal expansibility (α_p), isothermal compressibility (κ_T), and internal pressure (π_T):

$$\alpha_p = -\frac{1}{\rho}\left(\frac{\partial\rho}{\partial T}\right)_p \tag{28}$$

$$\kappa_T = \frac{1}{\rho}\left(\frac{\partial\rho}{\partial p}\right)_T \tag{29}$$

$$\pi_T = T\left(\frac{\kappa_T}{\alpha_p}\right)_T - p \tag{30}$$

4. Results and Discussion

4.1. Thermophysical properties atp = 0.1 MPa

In this section, experimental data of ρ, u, n_D, $C_{p,m}$, γ, and η at pressure of 0.1 MPa and temperatures from 278.15 to 338.15 K are presented, modelled, and discussed. Tables S1 and S2 report all data and Table 3 lists those at 298.15 K.

For both systems, the ρ measured at 0.1 MPa was lower than that of water. However, only LCM2 could be adequately separated in a liquid–liquid equilibrium with an aqueous phase. The ρ of the mixture with M ranged from 909.68 to 954.54 kg·m^{-3} and LCT was 40 kg·m^{-3} denser throughout the T range. A liquid can be considered as a continuous space that contains holes so that the volumetric behavior of the former will be the result of how different variables affect the latter. The flatter structure of T compared to the cycle of M would justify the need for a larger hole in the LCM2 mixture.

Fig. 1a shows the experimental ρ values at different T and those obtained with the linear correlation. The coefficients of the latter are listed in Table 4.

Having validated thermodynamic models that allow predicting property values under any composition, pressure, or temperature condition is a very useful tool. Here, we estimated the ρ with the PC-SAFT EoS (eq. 1–9) and compared these values with those experimental ones. The parameters of the pure compounds are listed in Table 5 and that of the binary interaction was null ($k_{ij} = 0$). The model predicted this property very well (Fig. S1) with mean relative deviations of 0.54 % for LCM2, and 0.46 % for LCT.

The propagation of sound is favored in more compact materials, so u is indicative of the structuring of the fluid. For LCT mixture, these data were a 2.5 % higher than those determined for LCM2, in agree with the above volumetric results. The increase in thermal agitation with increasing T represents a decrease in compaction and, consequently, a decrease in u. The decrease was linear as shown in Table 4 and Fig. 1b. The capacity of the liquid to compress under isentropic conditions or isentropic compressibility (κ_S) was calculated from ρ and u data at similar p and T. Also, an estimation of the free intermolecular length (L_f) was made from κ_S and the constant of Jacobson (K) [38]. The equations used are:

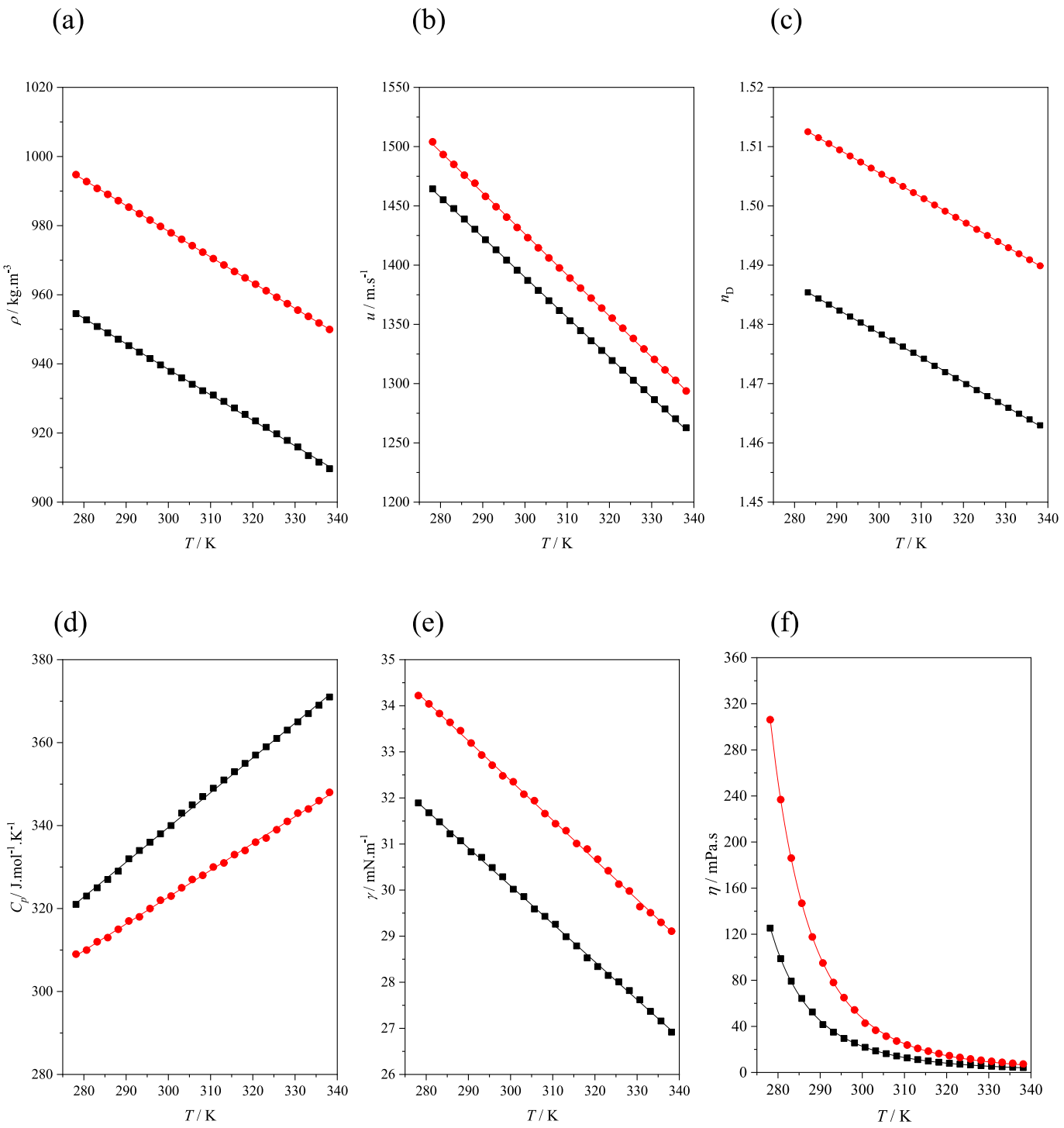

Fig. 1. Thermophysical properties of the studied mixtures as a function of temperature, T. (a), density, ρ; (b), speed of sound, u; (c), refraction index, n_D; (d), isobaric molar heat capacity, $C_{p,m}$; (e), surface tension, γ; (f), dynamic viscosity, η. (■), Lidocaine:camphor:l-menthol (1:1:2); (●), lidocaine:camphor:thymol (1:1:1). Points, experimental data; lines, correlated values.

$$\kappa_S = \frac{1}{\rho u^2} \tag{25}$$

$$L_f = K\sqrt{\kappa_S} = (91.368 + 0.3565\,T) \bullet 10^{-8}\sqrt{\kappa_S} \tag{26}$$

The κ_S values were higher for the mixture with M and increased with T due to the increase of the thermal motion (Table 3, Fig. S2a). The temperature coefficients of this property ($\partial\kappa_S/\partial T$) were 3.345 and 3.033 $TPa^{-1}\cdot K^{-1}$ for LCM2, and LCT, respectively. Moreover, L_f ranged from 0.421 to 0.556 Å for the mixture with M, and from 0.402 to 0.531 Å for that with T.

On the other hand, the propagation of light is favored in less compact materials, so n_D is also indicative of the structuring of the fluid. This property is defined as the ratio between the speed of light in the vacuum to that in the fluid. Then, the less compact fluid, the lower index. The results coincided with the previous ones, with LCT being the most compact mixture. The $n_D - T$ correlation was also a straight line with a negative slope (Table 4, Fig. 1c). An estimate of polarizability of the fluid, which is related to the hard-core volume, can be made from n_D and

Table 4
Fit parameters (A_Y, B_Y, C_Y) and the regression coefficients, R^2, for the thermophysical properties at$p = 0.1$ MPa of the studied mixtures.

Property	Mixture	A_Y	B_Y	C_Y	R^2
Density ρ^a/ kg·m^{-3}	lidocaine:camphor:l-menthol (1:1:2)	1160.05	–0.7387		0.99955
	lidocaine:camphor:thymol (1:1:1)	1201.57	–0.7440		0.99999
Speed of sound u^a/ m·s^{-1}	lidocaine:camphor:l-menthol (1:1:2)	2402.28	–3.3750		0.99987
	lidocaine:camphor:thymol (1:1:1)	2465.67	–3.4645		0.99986
Refraction index n_D^a	lidocaine:camphor:l-menthol (1:1:2)	1.60164	$-4.10\cdot10^{-4}$		0.99988
	lidocaine:camphor:thymol (1:1:1)	1.62930	$-4.12\cdot10^{-4}$		0.99999
Isobaric molar heat capacity $C_{p,m}^a$/ J·mol^{-1}·K^{-1}	lidocaine:camphor:l-menthol (1:1:2)	88.028	0.8385		0.99930
	lidocaine:camphor:thymol (1:1:1)	128.64	0.6471		0.99913
Surface tensión γ^a/ mN·m^{-1}	lidocaine:camphor:l-menthol (1:1:2)	54.78	–0.0823		0.99944
	lidocaine:camphor:thymol (1:1:1)	58.19	–0.0860		0.99927
Dynamic viscosity η^b/ mPa·s	lidocaine:camphor:l-menthol (1:1:2)	0.04215	643.86	197.67	0.99984
	lidocaine:camphor:thymol (1:1:1)	0.02184	855.44	188.57	0.99990

$^aY = A_Y + B_Y T$; $^bY = A_Y \exp\left(\frac{B_Y}{T - C_Y}\right)$

ρ data calculating the molar refraction (R_m) with the equation of Lorentz-Lorentz [39]:

$$R_m = \left(\frac{n_D^2 - 1}{n_D^2 + 2}\right)\frac{M}{\rho} \quad (27)$$

The R_m values were highest for the mixture with T. At 298.15 K, they are listed in Table 3 and as function of T are shown in Fig. S2b. The influence of T on R_m was small for both systems. The temperature coefficients ($\partial R_m/\partial T$) were $2.783\cdot10^{-3}$ and $3.787\cdot10^{-3}$ cm^3·mol^{-1}·K^{-1} for LCM2, and LCT, respectively. From R_m definition, the size of the holes or free volume (f_m) is calculated as the difference between the molar volume and molar refraction. As expected, data of the mixture with M were higher than those of with T and increased with T (Table 3, Fig. S2c). At 298.15 K, the percentages of unoccupied volume were 71.6 % for LCM2, and 70.3 % for LCT.

On average, the $C_{p,m}$ of the mixture with M was 5 % higher than that of the mixture with T, and this difference increased with T (Fig. 1d). The higher the temperature, the greater the ability of the fluids to accumulate energy. For most of them, the increase follows a linear equation. Table 3 lists the coefficients for our mixtures. Our experimental data were compared with those calculated with the correlation of Taherzadeh et al. (eq. 12–13) whose uncertainty estimated was 4.7 %. For this, the values of p_c and ω of the mixtures were needed and can be estimated with the Lee-Kesler (LK) mixing rules (14–19). For our ternary eutectic mixtures, we used the Excel worksheet provided by Boublia et al. [35]. The model underestimated $C_{p,m}$ for the mixture with M and slightly overestimated that of the mixture with T. The deviations were 5.5 % and 0.9 % for LCM2 and LCT, respectively. This property was also modeled with PC-SAFT (eq. 1–9). The EoS well predicted $C_{p,m}$ for both mixtures with deviations of 2.8 % for LCM2 and 3.1 % for LCT. The trends were similar to the above correlation (Fig. S1b).

Table 5
PC-SAFT parameters used to model the studied mixtures. The type 2B (one donor and one acceptor site) was considered as association scheme.

Compound	m	σ/ Å	ε/ K	$\kappa^{A_iB_i}$	$\varepsilon^{A_iB_i}$/ K
Lidocaine [a]	6.320	3.770	285.85	0.01	2798.5
Camphor [b]	3.583	3.984	283.50	0.01	2662.3
Thymol [c]	4.012	3.816	290.22	0.0616	1660.0
L-menthol [c]	4.152	3.903	262.40	0.0996	1785.6

[a] Ref. [19]; [b] Ref. [21]; [c] Ref. [37].

The movement of a molecule from the bulk of the liquid to the air–liquid interface implies an energy contribution, which is higher at higher cohesion between the molecules. The γ is a property indicative of this molecular cohesion. In a similar way to what was found with the properties previously studied, the measured γ data indicated that the interactions in the LCT mixture were stronger than in LCM2. For the later, γ was 7.7 % lower than for first. A linear decrease with T was also observed because increasing thermal agitation decreases the ability to establish interactions (Table 5, Fig. 1e). From this relationship, the entropy of surface (ΔS_S) and the enthalpy of surface (ΔH_S) were calculated:

$$\Delta S_S = -\left(\frac{\partial\gamma}{\partial T}\right)_p \quad (27)$$

$$\Delta H_S = \gamma - T\left(\frac{\partial\gamma}{\partial T}\right)_p \quad (28)$$

The greater the cohesive forces in the fluid, the greater the values of the surface properties. A higher structuration was observed in the LCT mixture (Table 3). The T_c is a very interesting thermodynamic property in the study of fluids but difficult to determine experimentally. Failing that, previously validated EoS, group contribution methods, and $\gamma - T_c$ correlations can be used. Table S3 reports T_c values estimated from the PC-SAFT EoS (eq. 1–9), LK mixing rules (eq. 14–19), and Guggenheim and Eötvos correlations (eq. 20–21). For both mixtures, the values calculated with LK and Guggenheim equations were the highest. By averaging the values estimated with the other methods, T_c(LCM2) = 745 ± 5 K, and T_c(LCT) = 764 ± 3 K. In Table S3, p_c values from PC-SAFTand LK are also included. The differences between estimated data were higher than 1 MPa. Molecules become polarized as they move from the interior of the fluid to the interface as their force field changes. Then, $\gamma - n_D$ relationship could be expected. Papazian proposed a linear equation between γ and a function of the n_D (eq. 22). A very high linearity was found for our mixtures with regression coefficients higher than 0.999. The fitting coefficients are listed in Table S4.

Viscosity is the resistance of any fluid to movement. Mainly, it depends on two factors: steric hindrance due to the geometry of the molecules, and intermolecular interactions. A high value may be beneficial for some applications as lubrication but is a drawback in those in which

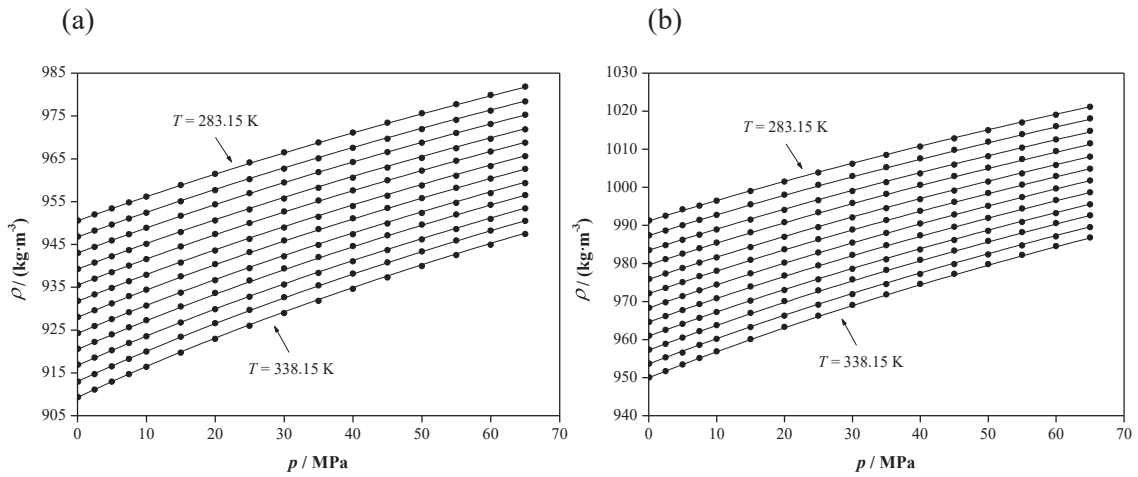

Fig. 2. Density, ρ, of the studied mixtures as a function of temperature, T, and pressure, p. (a), Lidocaine:camphor:l-menthol (1:1:2); (b), lidocaine:camphor:thymol (1:1:1). Points, experimental data; lines, correlated values (eq. 19–21).

the fluid acts as solvent. The value of 100 mPa·s has been established as the maximum value that ensures the proper operation of the equipment [40]. Our studied mixtures exhibited a η lower than that maximum value at T greater than 290 K. The LCT system was more viscous than LCM2, from 2.44 times at 278.15 K to 1.74 times at 338.15 K. The η decreased exponentially with increasing T as Fig. 1f shows. The coefficients of the equation used (eq. 11) are listed in Table 5. At $T\rightarrow\infty$, the interactions are completely prevented so the A_Y coefficient would be indicative of the steric hindrance due to the size and shape of the molecules. Additionally, the activation energy for viscous flow ($E_{a,\eta}$), measure of the strength of intermolecular interactions, is calculated from B_Y and C_Y according to the following equation [41]:

$$E_{a,\eta} = R\left(\frac{\partial \ln\eta}{\partial\left(\frac{1}{T}\right)}\right) = R\frac{B}{\left(\frac{C^2}{T^2} - \frac{2C}{T} + 1\right)} \quad (29)$$

Table 3 lists the $E_{a,\eta}$ data at 298.15 K and Fig. S2d displays those at different T. From A_Y and $E_{a,\eta}$ data, it can be seen that LCM2 exhibited the highest steric hindrance and LCT showed the strongest interactions. According to the measured η values, the second factor predominated over the first in our systems throughout the T range. Different authors have proposed a $\eta - \gamma$ relationship. In this work, we applied the Pelofsky and Murkerjee equations (eq. 23,24). Both correlations showed a good linearity for our mixtures. The coefficients are listed in Table S4.

No data were found in the literature of any of the thermophysical properties measured in this work for the LCM2 and LCT ternary systems. Nevertheless, a comparison with the results obtained previously by us for the LM2, CM2, LT, and CT binary systems can be performed [19–21]. The ρ and properties related to the compaction of the system were similar for the LM2 and LCM2 mixtures, and these values were higher than for CM2. The results showed that the influence of L on CM2 was greater than C on LM2. Also, η and $E_{a,\eta}$ were similar for CM2 and LCM2 and much lower than those of LM2. This fact could indicate that C hindered the interactions between L and M. In relation to the systems with T, data of the properties of the ternary mixture were intermediate with respect to those of the corresponding binaries. This result showed that the effect of L on CT compaction was similar to that of C on LT. Furthermore, the decrease of η in the LCT system was less pronounced than in LCM, probably because L interacted more strongly with T than with M. The latter agreed with studies carried out with NMR techniques [20].

Table 6
Parameters of the Tait equation (eq. 10–12) and the mean relative deviations of the studied mixtures.

	Lidocaine:camphor:l-menthol (1:1:2)	Lidocaine:camphor:thymol (1:1:1)
A_0/ kg·m^{-3}	1167.26	1253.35
A_1/ kg·m^{-3}·K^{-1}	–0.7785	–1.0736
A_1/ kg·m^{-3}·K^{-2}	$4.60\cdot10^{-5}$	$5.22\cdot10^{-4}$
C	0.0724	0.0727
B_0/ MPa	259.99	400.11
B_1/ MPa·K^{-1}	–0.4484	–1.2444
B_2/ MPa·K^{-2}	$-1.90\cdot10^{-4}$	$1.03\cdot10^{-3}$
$MRD^a(\rho)$/%	0.12	0.13

$^a MRD(\rho) = \frac{100}{n}\sum_{i=1}^{n}\left|\frac{\rho_{i,cal} - \rho_{i,exp}}{\rho_{i,exp}}\right|$

4.2. Volumetric properties under pressure

The ρ of the LCM2 and LCT mixtures at pressures from 0.1 to 65 MPa, and temperatures from 283.15 to 338.15 K were determined. From these values, derived properties as isobaric expansibility (α_p), isothermal compressibility (κ_T), and internal pressure (π_T), were calculated. All data are reported in Table S5–S8 and those for 0.1 MPa and 298.15 K are included in Table 3. No data for these ternary mixtures were found in the literature. Nevertheless, $p\rho T$ values of the binary CM2 and CT were published by our group at similar p and T ranges. So, a comparison between the volumetric behaviour of both type of systems can be performed.

The mixture with thymol was 40 kg·m^{-3} denser than that of l-menthol for any p and T. The higher ρ would be related to the planar configuration of the aromatic ring of thymol, and with stronger L-T interactions. Comparing with the corresponding binary mixtures, the incorporation of L into the system increased the ρ value. On average, ρ of LCM2 was 2.83 % greater than that of CM2, and ρ of LCT was 1.22 % greater than that of CT. The effect of L on ρ was smaller with increasing p. Again, the density was predicted with PC-SAFT EoS (eq. 1–9) and compared to measurements in similar way that above. The values provided by the model were slightly greater than the experimental ones and the relative mean deviations were$MRD(\rho)$ = 1.34 % and 1.10 % for LCM2, and LCT, respectively. No trends in the deviations with T were observed but they increased with p (fig. S1a). Despite that, the low $MRD(\rho)$ values do not justify a no-null k_{ij}. Fig. 2 shows the experimental

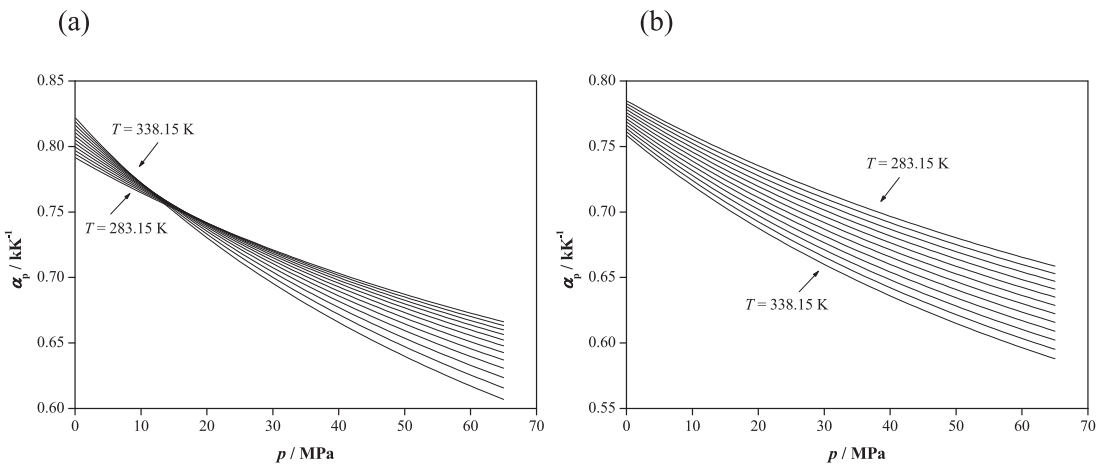

Fig. 3. Isobaric expansibility, α_p, of the studied mixtures as a function of temperature, T, and pressure, p. (a), Lidocaine:camphor:l-menthol (1:1:2); (b), lidocaine:camphor:thymol (1:1:1). Points, experimental data; lines, correlated values (eq. 28).

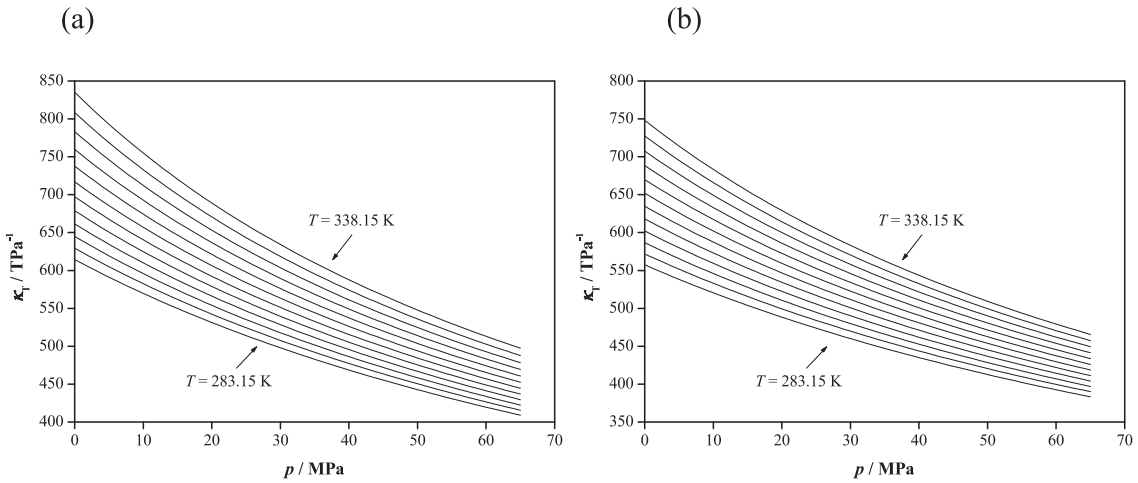

Fig. 4. Isothermal compressibility, κ_T, of the studied mixtures as a function of temperature, T, and pressure, p. (a), Lidocaine:camphor:l-menthol (1:1:2); (b), lidocaine:camphor:thymol (1:1:1). Points, experimental data; lines, correlated values (eq. 29).

ρ as a function of p at each T as well as those values obtained with the Tait equation (eq. 25–27). The coefficients of this correlation for both mixtures are reported in Table 6.

The effect of T on ρ was quantified with the α_p (eq. 28). The calculated values ranged from 0.607 to 0.822 kK^{-1} for LCM2 and from 0.588 to 0.785 kK^{-1} for LCT, showing that the first mixture was less compact. As expected, this property decreased with increasing p due to the decrease in the free volume of the system. On the other hand, an anomalous behavior with T was observed. For LCM2, the temperature coefficient was positive at pressures below 10 MPa and negative at pressures above 25 MPa (Fig. 3a). For LCT, this coefficient was negative at any p (Fig. 3b). This decrease in α_p with an increase in T has been related to the existence of strong interactions [42] so that the more condensed a fluid is, the lower the pressure value at which this phenomenon appears. It should be noted that in the CM2 and CT binary mixtures, the α_p increased with T throughout the p range. From this, it can be deduced that the presence of lidocaine causes a high structuring in the mixtures. Moreover, the κ_T (eq. 29) allows to estimate the effect of p on ρ. Again, the higher values were those of the mixture with M. They were from 408.99 to 834.48 TPa^{-1} for LCM2, and from 383.25 to 747.60 TPa^{-1} for LCT. As usual, this property increased with T and decreased with p (Fig. 4). An inverse linearity between κ_T and p was found. For both systems, the $(1/\kappa_T)$–p representation was a straight line ($R^2 = 1$) of slope$m$ = 12.5. This linearity was already found for CM2 and CT mixtures and was in accordance with that published by Wilhelm [43].

The π_T is a property related to the strength of the interactions present in a fluid and is calculated with the eq. (30). The stronger the interactions, the greater the π_T data. The calculated values ranged from 332.90 to 396.29 MPa for LCM2, and from 342.79 to 421.47 MPa for LCT. They were also greater than the corresponding binary mixtures without L. The π_T increased with p because intermolecular interactions are favored by decreasing free volume (Fig. 5a, 5b). On the other hand, the π_T decreased monotonically with increasing T (Fig. 5c, 5d), which indicated a prevalence of hydrogen bonds over van der Waals interactions [44]. From all this, it can be deduced that the presence of L in the system contributed to structuring the fluid and that the L-T interactions were greater than the L-M interactions. These results were in agreement with those previously found by us using NMR techniques [20].

The cohesive energy density (CED) can be estimated from thermodynamical models previously validated as PC-SAFT EoS, and can be written as the sum of two contributions [45,46]. The first (δ_V^2) is related to van der Waals interactions and can be calculated as the square root of the internal pressure. The second (δ_R^2) is related to the interactions of chemical character, and consequently, can be calculated from the difference between CED and π_T. Based on all of the above, δ_R^2 of LCT was expected to be the highest value. At 298.15 K and 0.1 MPa, δ_R^2=47.11

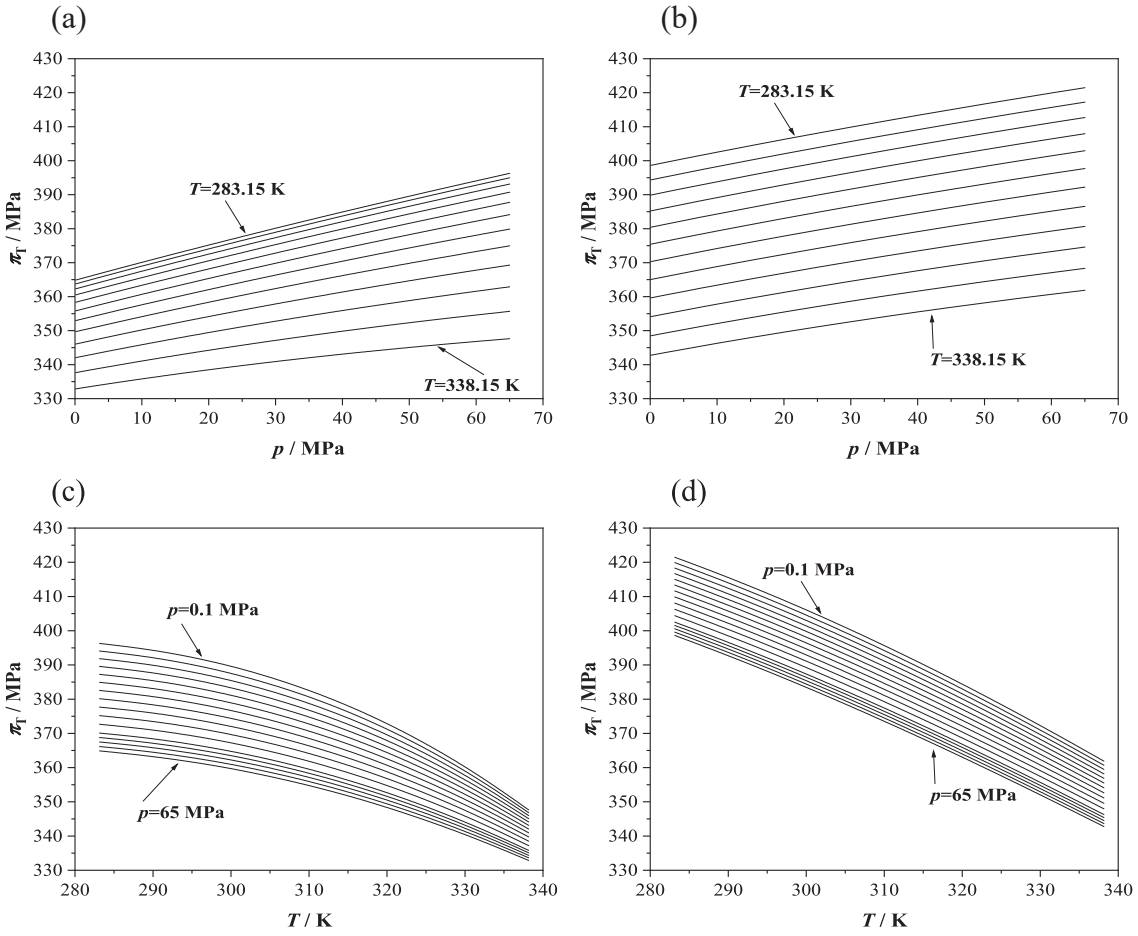

Fig. 5. Internal pressure, π_T, of the studied mixtures as a function of temperature, T, and pressure, p. (a,c), Lidocaine:camphor:l-menthol (1:1:2); (b,d), lidocaine:camphor:thymol (1:1:1). Points, experimental data; lines, correlated values (eq. 30).

MPa for LCM2, and δ_R^2 = 60.37 MPa for LCT. These values were also higher than the corresponding binary mixtures [21].

5. Conclusions

In this work, the thermophysical characterization of two hydrophobic eutectic solvents was performed. They were the ternary mixtures lidocaine:camphor:l-menthol (1:1:2) (LCM2), and lidocaine:camphor:thymol (1:1:1) (LCT). For this study, the density, speed of sound, refractive index, isobaric molar heat capacity, surface tension, and dynamic viscosity were measured at 0.1 MPa and from 278.15 to 338.15 K. Furthermore, the volumetric behavior in a pressure range of 0.1 to 65 MPa, and at temperatures from 283.15 to 338.15 K was determined and evaluated. From these data, several derived properties and correlations were presented. Finally, the PC-SAFT equation of state was validated for both systems. The results were analyzed and compared with those previously obtained for the corresponding binary mixtures.

The LCT was the most dense, compact, structured and viscous mixture. Also, its critical temperature estimated from different equations was higher than that of LCM2. The $C_{p,m}$ values from the Taherzadeh correlation were close to those measured, with deviations of 5.5 % and 0.9 % for LCM2 and LCT, respectively. High linearities were found in the correlations between the surface tension and refractive index, and viscosity. The PC-SAFT model adequately predicted ρ throughout the range of p and T with a mean relative deviation from the experimental values of less than 1.4 %. For $C_{p,m}$ at 0.1 MPa, the deviation was less than 3.1 %. The interactions between L and T were stronger than those with M. The incorporation of C to the binary mixtures hindered the interactions of L with both terpenes, especially those between L and M.

CRediT authorship contribution statement

Mónica Sancho-Blasco: Resources, Methodology, Data curation. **Jorge L. Pastor:** Methodology, Data curation. **José Muñoz-Embid:** Writing – original draft, Formal analysis. **Carlos Lafuente:** Writing – original draft, Validation. **Manuela Artal:** Writing – review & editing, Writing – original draft, Supervision.

Declaration of competing interest

The authors declare that they have no known competing financial interests or personal relationships that could have appeared to influence the work reported in this paper.

Acknowledgments

PLATON research group acknowledges financial support from Gobierno de Aragón and Fondo Social Europeo “Construyendo Europa desde Aragón”_E31_23R.

Appendix A. Supplementary data

Supplementary data to this article can be found online at https://doi.org/10.1016/j.molliq.2024.126655.

Data availability

The authors confirm that the data supporting the findings of this study are available within the article and its supplementary materials.

References

[1] L.Z. Benet, The Role of BCS (Biopharmaceutics Classification System) and BDDCS (Biopharmaceutics Drug Disposition Classification System) in Drug Development, J. Pharm. Sci. 102 (2013) 34–42, https://doi.org/10.1002/jps.23359.

[2] L. Kumari, Y. Choudhari, P. Patel, G. Das Gupta, D. Singh, J.M. Rosenholm, K. K. Bansal, B. Das Kurmi, Advancement in Solubilization Approaches: A Step towards Bioavailability Enhancement of Poorly Soluble Drugs, Life 13 (2023) 1099, https://doi.org/10.3390/life13051099.

[3] M.S. Kinch, Z. Kraft, T. Schwartz, 2023 in review: FDA approvals of new medicines, Drug Discov. Today 29 (2024) 103966, https://doi.org/10.1016/j.drudis.2024.103966.

[4] M. Akbarian, S.-H. Chen, Instability Challenges and Stabilization Strategies of Pharmaceutical Proteins, Pharmaceutics 14 (2022) 2533, https://doi.org/10.3390/pharmaceutics14112533.

[5] F. Guthrie, LII. *On eutexia*, The London, Edinburgh, and Dublin Philosophical Magazine and Journal of Science 17 (1884) 462–482. Doi: 10.1080/14786448408627543.

[6] A.P. Abbott, D. Boothby, G. Capper, D.L. Davies, R.K. Rasheed, Deep Eutectic Solvents formed between choline chloride and carboxylic acids: Versatile alternatives to ionic liquids, J. Am. Chem. Soc. 126 (2004) 9142–9147, https://doi.org/10.1021/ja048266j.

[7] E.L. Smith, A.P. Abbott, K.S. Ryder, Deep Eutectic Solvents (DESs) and Their Applications, Chem. Rev. 114 (2014) 11060–11082, https://doi.org/10.1021/cr300162p.

[8] M.A.R. Martins, S.P. Pinho, J.A.P. Coutinho, Insights into the Nature of Eutectic and Deep Eutectic Mixtures, J. Solution Chem. (2018), https://doi.org/10.1007/s10953-018-0793-1.

[9] L. Sportiello, F. Favati, N. Condelli, M. Di Cairano, M.C. Caruso, B. Simonato, R. Tolve, F. Galgano, Hydrophobic deep eutectic solvents in the food sector: Focus on their use for the extraction of bioactive compounds, Food Chem. 405 (2023), https://doi.org/10.1016/j.foodchem.2022.134703.

[10] M.M. Abdelquader, S. Li, G.P. Andrews, D.S. Jones, Therapeutic deep eutectic solvents: A comprehensive review of their thermodynamics, microstructure and drug delivery applications, European Journal of Pharmaceutics and Biopharmaceutics 186 (2023) 85–104, https://doi.org/10.1016/j.ejpb.2023.03.002.

[11] C. Ferreira, M. Sarraguça, A Comprehensive Review on Deep Eutectic Solvents and Its Use to Extract Bioactive Compounds of Pharmaceutical Interest, Pharmaceuticals 17 (2024), https://doi.org/10.3390/ph17010124.

[12] S. Kalantri, A. Vora, Eutectic solutions for healing: a comprehensive review on therapeutic deep eutectic solvents (TheDES), Drug Dev. Ind. Pharm. 50 (2024) 387–400, https://doi.org/10.1080/03639045.2024.2345131.

[13] J.L. Shamshina, R.D. Rogers, Ionic Liquids: New Forms of Active Pharmaceutical Ingredients with Unique, Tunable Properties, Chem. Rev. 123 (2023) 11894–11953, https://doi.org/10.1021/acs.chemrev.3c00384.

[14] S. Kapre, S.S. Palakurthi, A. Jain, S. Palakurthi, DES-igning the future of drug delivery: A journey from fundamentals to drug delivery applications, J. Mol. Liq. 400 (2024) 124517, https://doi.org/10.1016/j.molliq.2024.124517.

[15] X. Yang, X. Wei, Y. Mu, Q. Li, J. Liu, A review of the mechanism of the central analgesic effect of lidocaine, Medicine 99 (2020) e19898.

[16] A. Scriabini, Discovery and development of major drugs currently in use, in: Pharmaceutical Innovation: Revolutionizing Human Health, Chemical Heritage Press, Philadelphia, PA, 1999: pp. 148–270.

[17] B. Mir, S. Bakhtawar, M. Naz, B. Uroos, F.S. Ali, Pharmaceutical applications of lidocaine-based ionic liquids – A remarkable innovation in drug delivery, J Mol Liq 397 (2024) 124052, https://doi.org/10.1016/j.molliq.2024.124052.

[18] S. Li, M.M. Abdelquader, G.P. Andrews, D.S. Jones, Towards a greater understanding of the deep eutectic phenomenon through examination of the lidocaine-NSAID therapeutic deep eutectic systems, Eur. J. Pharm. Biopharm. 200 (2024) 114329, https://doi.org/10.1016/j.ejpb.2024.114329.

[19] M. Molero-Sangüesa, I. Jiménez-Omeñaca, F. Bergua, H. Artigas, C. Lafuente, M. Artal, Thermophysical properties of lidocaine:thymol or L-menthol eutectic mixtures, J. Taiwan Inst. Chem. Eng. 163 (2024), https://doi.org/10.1016/j.jtice.2024.105631.

[20] N. Padilla, I. Delso, F. Bergua, C. Lafuente, M. Artal, Characterization of camphor: thymol or dl-menthol eutectic mixtures; Structure, thermophysical properties, and lidocaine solubility, J. Mol. Liq. 405 (2024), https://doi.org/10.1016/j.molliq.2024.125069.

[21] V. Hernández-Serrano, J. Muñoz-Embid, F. Bergua, C. Lafuente, M. Artal, pVT behaviour of hydrophilic and hydrophobic eutectic solvents, J. Mol. Liq. 382 (2023), https://doi.org/10.1016/j.molliq.2023.122019.

[22] M. Taherzadeh, R. Haghbakhsh, A.R.C. Duarte, S. Raeissi, Estimation of the heat capacities of deep eutectic solvents, J. Mol. Liq. 307 (2020) 112940, https://doi.org/10.1016/j.molliq.2020.112940.

[23] E.A. Guggenheim, The principle of corresponding states, J. Phys. Chem. 13 (1945) 253–261.

[24] J.L.L. Shereshefsky, Surface tension of saturated vapors and the equation of Eötvos, J. Phys. Chem. 35 (1930) 1712–1720, https://doi.org/10.1021/j150324a014.

[25] H.A. Papazian, Correlation of surface tension between various liquids, J. Am. Chem. Soc. 93 (1971) 5634–5636, https://doi.org/10.1021/ja00751a008.

[26] A.H. Pelofsky, Surface Tension-Viscosity Relation for Liquids, J. Chem. Eng. Data 11 (1966) 394–397, https://doi.org/10.1021/je60030a031.

[27] J. Gross, G. Sadowski, Perturbed-chain SAFT: An equation of state based on a perturbation theory for chain molecules, Ind. Eng. Chem. Res. 40 (2001) 1244–1260, https://doi.org/10.1021/ie0003887.

[28] J. Gross, G. Sadowski, Application of the perturbed-chain SAFT equation of state to associating systems, Ind. Eng. Chem. Res. 41 (2002) 5510–5515, https://doi.org/10.1021/ie010954d.

[29] W.G. Chapman, G. Jackson, K.E. Gubbins, Phase equilibria of associating fluids, Mol. Phys. 65 (1988) 1057–1079, https://doi.org/10.1080/00268978800101601.

[30] J.A. Barker, D. Henderson, Perturbation Theory and Equation of State for Fluids. II. A Successful Theory of Liquids, J. Chem. Phys. 47 (1967) 4714–4721, https://doi.org/10.1063/1.1701689.

[31] J.A. Barker, D. Henderson, Perturbation Theory and Equation of State for Fluids: The Square-Well Potential, J. Chem. Phys. 47 (1967) 2856–2861, https://doi.org/10.1063/1.1712308.

[32] H. Vogel, The temperature dependence law of the viscosity of fluids, Physikalische Zeitschrift 22 (1921) 645–646.

[33] G.S. Fulcher, Analisis of recent measurements of the viscosity of glasses, J. Am. Ceram. Soc. 8 (1925) 339–355, https://doi.org/10.1111/j.1151-2916.1925.tb16731.x.

[34] G. Tammann, W. Hesse, The dependancy of viscosity on temperature of supercooled liquids, Z. Anorg. Allg. Chem. 156 (1926) 245–257.

[35] A. Boublia, T. Lemaoui, G. Almustafa, A.S. Darwish, Y. Benguerba, F. Banat, I. M. AlNashef, Critical Properties of Ternary Deep Eutectic Solvents Using Group Contribution with Extended Lee-Kesler Mixing Rules, ACS Omega 8 (2023) 13177–13191, https://doi.org/10.1021/acsomega.3c00436.

[36] J.H. Dymond, R. Malhotra, The Tait equation: 100 years on, Int. J. Thermophys. 9 (1988) 941–951, https://doi.org/10.1007/BF01133262.

[37] M.A.R. Martins, E.A. Crespo, P.V.A. Pontes, L.P. Silva, M. Bülow, G.J. Maximo, E.A. C. Batista, C. Held, S.P. Pinho, J.A.P. Coutinho, Tunable Hydrophobic Eutectic Solvents Based on Terpenes and Monocarboxylic Acids, ACS Sustain. Chem. Eng. 6 (2018) 8836–8846, https://doi.org/10.1021/acssuschemeng.8b01203.

[38] B. Jacobson, Ultrasonic Velocity in Liquids and Liquid Mixtures, J. Chem. Phys. 20 (1952) 927–928, https://doi.org/10.1063/1.1700615.

[39] A. McNaught, A.D.; Wilkinson, Compendium of Chemical Terminology, Iupac Recommendations, Second ed., Blackwell Science, Cambridge, 1997.

[40] D.J.G.P. Van Osch, C.H.J.T. Dietz, J. Van Spronsen, M.C. Kroon, F. Gallucci, M. Van Sint Annaland, R. Tuinier, A Search for Natural Hydrophobic Deep Eutectic Solvents Based on Natural Components, ACS Sustain Chem Eng 7 (2019) 2933–2942, https://doi.org/10.1021/acssuschemeng.8b03520.

[41] C. Florindo, L.C.C. Branco, I.M.M. Marrucho, Development of hydrophobic deep eutectic solvents for extraction of pesticides from aqueous environments, Fluid Phase Equilib. 448 (2017) 135–142, https://doi.org/10.1016/j.fluid.2017.04.002.

[42] J. Troncoso, C.A. Cerdeiriña, P. Navia, Y.A. Sanmamed, D. González-Salgado, L. Romaní, Unusual Behavior of the Thermodynamic Response Functions of Ionic Liquids, J. Phys. Chem. Lett. 1 (2010) 211–214, https://doi.org/10.1021/jz900049g.

[43] E. Wilhelm, Pressure dependence of the isothermal compressibility and a modified form of the Tait equation, J. Chem. Phys. 63 (1975) 3379–3381, https://doi.org/10.1063/1.431774.

[44] V.N. Kartsev, S.N. Shtykov, K.E. Pankin, D.V. Batov, Intermolecular forces and the internal pressure of liquids, J. Struct. Chem. 53 (2012) 1087–1093, https://doi.org/10.1134/S0022476612060108.

[45] J.H. Hildebrand, Solubility of non-electrolytes. By J. H. Hildebrand, Ph.D. 2nd ed. Pp. 203. New York: Reinhold Publishing Corp., London: Chapman & Hall, Ltd., 1936. 22s. 6d, Journal of the Society of Chemical Industry 55 (1936) 665–665. Doi: 10.1002/jctb.5000553408.

[46] J.M.S.E.B. Bagley, T.P. Nelson, Three-dimensional solubility parameters and their relationship to internal pressure measurements in polar and hydrogen bonding solvents, J Paint Technol 43 (1971) 35–42.